Development 138, 3711-3721 (2011) doi:10.1242/dev.068270

Tcf/Lef repressors differentially regulate Shh-Gli target gene activation thresholds to generate progenitor patterning in the developing CNS

Hui Wang[1], Qiubo Lei[1,*], Tony Oosterveen[2], Johan Ericson[2] and Michael P. Matise[1,†]

SUMMARY

During neural tube development, Shh signaling through Gli transcription factors is necessary to establish five distinct ventral progenitor domains that give rise to unique classes of neurons and glia that arise in specific positions along the dorsoventral axis. These cells are generated from progenitors that display distinct transcription factor gene expression profiles in specific domains in the ventricular zone. However, the molecular genetic mechanisms that control the differential spatiotemporal transcriptional responses of progenitor target genes to graded Shh-Gli signaling remain unclear. The current study demonstrates a role for Tcf/Lef repressor activity in this process. We show that *Tcf3* and *Tcf7L2* (*Tcf4*) are required for proper ventral patterning and function by independently regulating two Shh-Gli target genes, *Nkx2.2* and *Olig2*, which are initially induced in a common pool of progenitors that ultimately segregate into unique territories giving rise to distinct progeny. Genetic and functional studies in vivo show that Tcf transcriptional repressors selectively elevate the strength and duration of Gli activity necessary to induce Nkx2.2, but have no effect on Olig2, and thereby contribute to the establishment of their distinct expression domains in cooperation with graded Shh signaling. Together, our data reveal a Shh-Gli-independent transcriptional input that is required to shape the precise spatial and temporal response to extracellular morphogen signaling information during lineage segregation in the CNS.

KEY WORDS: Gli proteins, Morphogen signaling, Patterning, Tcf proteins, Gene expression, Spinal cord, Mouse, Chick

INTRODUCTION

The specification and patterning of neuronal subtypes in the ventral neural tube by the secreted sonic hedgehog (Shh) protein has emerged as a paradigm for studies of morphogenetic signaling (Dessaud et al., 2008; McMahon et al., 2003). Shh from the notochord and floorplate is required to establish five discrete ventral progenitor domains that give rise to unique classes of neurons and glia that emerge in specific dorsoventral (DV) positions. Neuronal progenitors and their postmitotic progeny can be identified by the expression of distinct sets of transcription factor proteins, which play important roles in both the establishment of unique territories and in promoting cellular differentiation programs (Dessaud et al., 2008; Lee and Pfaff, 2001). Five neuronal classes and one non-neuronal class have been identified on this basis, termed V0, V1, V2, MN, V3 and FP, from dorsal to ventral (Ericson et al., 1997b; Ericson et al., 1992; Jessell, 2000; Matise and Joyner, 1997). These are generated from progenitors that also display distinct transcription factor profiles in specific domains in the ventricular zone (VZ) (correspondingly termed p0, p1, p2, pMN, p3) (Briscoe et al., 2000). In addition to the spatial pattern, there is also a temporal sequence of ventral progenitor gene activation. The earliest ventral genes to appear are Nkx6.2 and Nkx6.1, which later demarcate the p1 and p2 domains, respectively, followed by Olig2 (pMN), Nkx2.2 (p3) and finally FoxA2 (FP) (Dessaud et al., 2008; Jeong and McMahon, 2005; Lek et al., 2010). A full understanding of how distinct cell fates are established therefore rests on determining the molecular genetic mechanisms that control the spatiotemporal transcriptional responses of progenitor target genes to graded Shh signaling information in ventral cells.

The three Gli family zinc-finger proteins are requisite downstream components of the Hedgehog (Hh) pathway that mediate the direct target gene transcriptional responses to this extracellular signaling protein (Dessaud et al., 2008; Jacob and Briscoe, 2003; Jiang and Hui, 2008; Ruiz i Altaba et al., 2003). Gli proteins are bi-functional transcription factors, dual activities of which are regulated by signaling status. In the absence of Hh, Gli proteins are proteolyzed either partially to form a transcriptional repressor (Gli3) or completely to be degraded (Gli1 and Gli2) (Pan et al., 2006; Pan and Wang, 2007). In the presence of Hh, Gli proteins are not proteolyzed and instead function as activators of Hh target genes (Jacob and Briscoe, 2003; Pan et al., 2006). These data suggest that inhibition of constitutive Gli protein proteolysis is a prerequisite for Gli activator (GliA) formation, and that the ratio of GliA to Gli repressors (GliR) reflects graded Shh signaling levels along the DV axis (Jacob and Briscoe, 2003; Ruiz i Altaba et al., 2003). In vivo transfection of GliA proteins at several distinct concentrations can induce a proportional induction of ventral progenitor genes along the DV axis, mirroring classical studies that established a correlation between Shh protein levels and positional marker gene induction in neural tube explant cultures (Ericson et al., 1997a; Lei et al., 2004; Stamataki et al., 2005). These data together support a model in which extracellular Shh levels and/or length of exposure are translated by graded Gli protein activities to

[1]Department of Neuroscience and Cell Biology, Robert Wood Johnson Medical School, University of Medicine and Dentistry of New Jersey, 675 Hoes Lane, Piscataway, NJ 08854, USA. [2]Department of Cell and Molecular Biology, Karolinska Institutet, P.O. Box 285, SE-171 77 Stockholm, Sweden.

*Present address: Sanofi-Aventis USA, 1041 Route 202-206, PO Box 6800, Bridgewater, NJ 08807, USA
†Author for correspondence (matisemp@umdnj.edu)

Accepted 22 June 2011

direct differential target gene responses in the nucleus (Dessaud et al., 2008; Ribes and Briscoe, 2009; Stamataki et al., 2005), and suggest that Shh-Gli target genes respond to a narrow range of Gli activity levels and are induced only after a given gene-specific threshold has been reached.

A key question that remains is how activation thresholds are set for distinct Shh-Gli target genes that appear at distinct times and locations along the DV axis. Because Shh can both inhibit GliR and promote GliA formation, the expression of Shh-Gli target genes could, in principle, be controlled by de-repression, direct activation, or a combination of both. In the developing spinal cord, gain- and loss-of-function studies demonstrate that although Gli proteins are sufficient to induce expression of many ventral progenitor genes, data from mouse mutants lacking specific Gli activities suggest that not all genes are equivalent in their requirement. For example, only some of the ventral cell types that do not form in *Shh* mutants, which retain high levels of Gli3R activity, are rescued in *Shh Gli3*, *Smo Gli3* and *Gli2 Gli3* double mutants that lack all Gli (GliA and GliR) activities (Bai et al., 2004; Lei et al., 2004; Litingtung and Chiang, 2000; Wijgerde et al., 2002). Specifically, the factors that define the three most ventral progenitor domains, FoxA2 (FP), Nkx2.2 (p3) and Olig2 (pMN) (from ventral to dorsal) all appear to require prior Shh-dependent repression of ventral *Gli3* expression (GliR activity) for their expression, but only Nkx2.2 and FoxA2 require GliA signaling (Bai et al., 2004; Lei et al., 2004). By contrast, de-repression appears to be sufficient for Olig2 induction (Bai et al., 2004; Lei et al., 2004) either by default or by unmasking an Shh-independent signaling activity, such as retinoic acid, that induces expression (Novitch et al., 2003; Pierani et al., 1999). Similarly, the Shh-dependent induction of another progenitor gene, *Nkx6.1* (Vokes et al., 2007), also appears to be regulated primarily by a de-repression rather than direct activation mechanism (Bai et al., 2004; Lei et al., 2004). These observations raise the possibility that distinct mechanisms control the threshold responses for target genes regulated by each Gli transcriptional activity.

In previous studies, we identified the cis-acting DNA regulatory module (CRM) that controls the p3-domain-restricted expression of Nkx2.2 in the ventral neural tube (Lei et al., 2006). We found that this CRM contained a single Gli binding site that was required for its expression. Two additional binding sites for Tcf proteins were also identified within a highly conserved region in close proximity (<100 bp) to the Gli site, and deletion of these sequences resulted in de-repression of *Nkx2.2 p3* CRM-driven reporter expression in dorsal progenitor territories. These data suggest that Nkx2.2 expression can be induced over a wide range of endogenous Gli levels in vivo in the absence of Tcf/Lef transcriptional input, arguing against the idea that its response is tuned to a specific, narrow Shh-Gli activity range. Furthermore, they raise the possibility that Tcf transcriptional repressor activity is involved in the establishment and/or maintenance of domain-restricted Nkx2.2 expression. In the current study, we addressed this question directly by examining the requirement of Tcf/Lef proteins for regulation of the differential expression of key Shh-Gli target genes in the ventral neural tube. Our analysis of progenitor domain formation in the spinal cord of *Tcf3* mutant embryos, *Tcf7l2* (hereafter referred to as *Tcf4*) mutant embryos and *Tcf3 Tcf4* double mutant embryos that lack all ventral Tcf/Lef activity reveals that loss of these factors results in ectopic Nkx2.2 expression in the dorsal pMN domain that is more severe in double mutants in which it is accompanied by a reduction in the number of Olig2+ pMN cells. Using genetic and functional approaches, we find that Tcf repressor (TcfR) activity elevates the Gli induction threshold for Nkx2.2, but has no effect on Olig2. Taken with genetic lineage tracing results, these findings suggest that, in the absence of Tcf repression, Nkx2.2 expression fails to be downregulated in many pMN cells as they segregate from a bi-potent p3/pMN progenitor pool that transiently co-expresses Olig2. Together, our results reveal an important function for Tcf repressor activity in establishing Shh-Gli induction thresholds for distinct target genes that is required for normal ventral patterning in the developing neural tube.

MATERIALS AND METHODS

Generation and analysis of transgenic and mutant mouse strains

All mouse strains were maintained on an outbred Swiss Webster background. The generation of targeted *Tcf3*, *Tcf7L2* (*Tcf4*), *Rosa26-floxed-stop-lacZ* and *Gli2* mutant mice has previously been described (Mo et al., 1997; Soriano, 1999). To generate transgenic constructs for *Nkx2.2*$^{p3\text{-}CRM}$*::Cre* mice, the *lacZ* gene in the previously identified 1.2-kb *Eco*RI-*Sac*II fragment *Nkx2.2 p3*-CRM (Lei et al., 2006) was replaced by a cDNA encoding the bacterial *Cre recombinase* gene. For *FoxA2*$^{FP\text{-}CRM}$*::Cre*, two fragments [‘A’ and ‘400’ from Sasaki and Hogan (Sasaki and Hogan, 1996)] that drive floor plate-specific expression were cloned upstream of *Cre*. Transgenic lines were generated using standard zygote DNA injection methods at the Transgenic Core Facility of the UMDNJ Cancer Institute. Two independent lines were generated for each construct.

In ovo electroporation and luciferase assays

Transfection of chick embryos using in ovo electroporation was performed as described (Lei et al., 2004). For in vivo measurements of *Nkx2.2* enhancer expression, the *Nkx2.2 p3*-CRM was cloned upstream of the firefly *luciferase* gene and a minimal human β-globin promoter in the promoter-less pGL3 vector. A construct encoding *Renilla* was used as an internal control and an pUC18 empty plasmid to balance final DNA concentrations. For concentration-dependent tests, reporter construct (*Nkx2.2*$^{p3\text{-}CRM}$*::luc*), effector constructs (GliA or TcfR) and internal transfection control constructs (Renilla) were electroporated at embryonic day (E) 2/Hamburger & Hamilton stage (HH) 12-13, returned to the incubator at 37°C, and collected 26 hours post-transfection (hpt) at stage 18-19. To test the temporal response, embryos were collected at 3-hour intervals at 12-27 hpt. Embryos were then removed from eggs, homogenized with 22 gauge 1.5 inch needles and lysed with Passive Lysis Buffer (Promega). Luciferase activity was recorded using Promega dual channel luciferase assay kit and a Turner Instruments T20 luminometer. Each assay was performed with three to four replicates for one point, and each separate experiment was replicated at least twice.

The mouse *Olig2*$^{pMN\text{-}CRM}$*::lacZ* construct was generated by subcloning a 2.2-kb genomic fragment located ~32 kb upstream of the Olig2 gene coding region into a plasmid vector containing *lacZ* and a minimal β-globin promoter.

ChIP and qPCR assay

Chromatin immunoprecipitation (ChIP) was performed on extracts from E10.5 mouse embryos (six embryos pooled, 200 μl cell lysate per assay). A ChIP-grade anti-Tcf3/4 mouse monoclonal antibody (Upstate Biotechnology) was used to precipitate DNA, and PCR was performed using the following primers flanking the known (*Nkx2.2*) and putative (*Olig2*) Tcf consensus binding sequences: *Nkx2.2*, 5′-AGTATGT-GACGTGGGTGACAATGG-3′ forward, 5′-GCCATGACAACTAGGG-ACAACCTT-3′ reverse; *Olig2*, 5′-GTTGTCTCTCTGGGTGGAAA-GAGG-3′ forward and 5′-GGTGGGAAACGACAATGGTCCTTC-3′ reverse. An anti-acetyl-histone H3 antibody (Upstate Biotechnology) was used as a positive control. A quantitative PCR (qPCR) assay was performed on E10.5 and E11.5 mouse embryos. For this, total RNA was extracted using Invitrogen TRIzol reagent and qPCR was performed on cDNA generated using Taqman reverse transcription reagents with *Gli1* primers and control 18s RNA primers (Applied Biosystems).

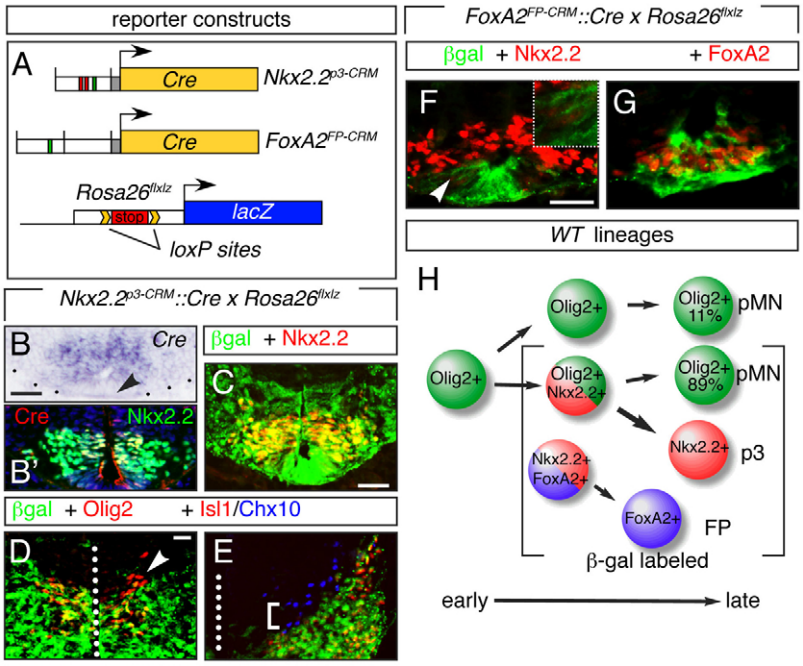

Fig. 1. Expression of an *Nkx2.2 p3* cis-regulatory module (CRM) in three distinct ventral lineages. (**A**) Schematic of the constructs used. Small green and red boxes indicate relative location of confirmed Gli and Tcf binding sites, respectively, for the first two constructs. Bottom figure shows the targeted *Rosa26 flox-stop-lacZ* (*flxlz*) reporter line. (**B**,**B'**) *Cre* mRNA (B) and protein (B′) expression driven by *Nkx2.2 p3*-CRM is restricted to Nkx2.2+ cells within the p3 domain at E10.5. Section in B′ is labeled by DAPI (blue channel). Note the absence of staining in the FP (arrowheads). Black dots indicate the spinal cord margin. (**C-E**) Mapping of β-gal expression from the *Rosa26*^{flxlz} line in transgenic mice expressing *Cre recombinase* from the *Nkx2.2 p3*-CRM. β-Gal expression is detected in FP, p3 (marked by Nkx2.2), pMN (marked by Olig2) cells and motoneurons (marked by Isl1), but not V2 cells (marked by Chx10; bracket). Arrowhead in D indicates subset of Olig2+ cells that do not co-express β-gal. Dotted lines in D and E indicate the central canal. (**F**,**G**) Mapping of β-gal expression from the *Rosa26*^{flxlz} locus in transgenic mice expressing *Cre recombinase* from the *FoxA2* floor plate (FP) CRM. β-Gal expression is detected in FoxA2+ FP cells but not Nkx2.2+ p3 cells. Weak Nkx2.2 expression can be detected in a few lateral FP cells (arrowhead and inset in F). (**H**) Model summarizing the results of lineage tracing using the *Nkx2.2 p3*-CRM and *FoxA2 FP*-CRM and integrating published expression and lineage data for Olig2 (see text). Nkx2.2 expression is activated in the progenitors of three distinct lineages in the neural tube but is only retained in the p3 domain (thicker arrow). Brackets indicate the sub-lineages expressing β-gal that derive from cells that activate *Nkx2.2 p3*-CRM. E10.5 embryos shown in all figures. Scale bars: 25 μm.

Immunostaining, in situ hybridization and quantification

Immunostaining and in situ hybridization were performed on frozen tissue sections as described (Lei et al., 2004). For all figures, three to five separate embryos and eight to ten sections were counted for each marker. For 5-bromo-2′-deoxyuridine (BrdU) staining, a single 5 μg/μl of BrdU in PBS was injected intraperitoneally prior to sacrifice. All images shown were taken from mid-thoracic levels unless otherwise noted. Statistical analysis was performed as described on cell count data using Student's *t*-test (Lei et al., 2006). For luciferase plots, a best-fit regression line was drawn in Microsoft Excel for each data set using two-period moving average.

RESULTS

An Nkx2.2 p3 enhancer is transiently activated in three ventral progenitor lineages

To study the dynamics of ventral progenitor segregation in the ventral neural tube, we used Cre-loxP-mediated fate mapping to determine the lineage relationships between the neuronal progenitors that activate expression of *Nkx2.2* and *FoxA2*. We generated stable transgenic lines using a previously identified *Nkx2.2* p3 cis-regulatory module (CRM) (Lei et al., 2006) and *FoxA2* floor plate (FP) CRM (Sasaki and Hogan, 1996) to drive *Cre recombinase*, and crossed these mice with the *ROSA26-floxed-stop-lacZ* (*flxlz*) conditional reporter line (Soriano, 1999) (Fig. 1A). Enhancer-driven *Cre* mRNA and protein expression in *Nkx2.2*$^{p3\text{-}CRM}$*::Cre* transgenics was restricted to p3 cells between E9.5 and E10.5, confirming that its activity faithfully mimics endogenous Nkx2.2 expression (Fig. 1B,B′; data not shown). When β-gal expression was examined in E9.5-11.5 embryos derived from *Nkx2.2*$^{p3\text{-}CRM}$*::Cre* × *ROSA26*^{flxlz} crosses, it was detected in FoxA2+ FP cells, Nkx2.2+ p3 cells and Olig2+ pMN cells, and in Isl1+ motoneurons (Fig. 1C-E; data not shown). Virtually no expression was found in p2 progenitors or Chx10 (Vsx2)+ progeny (Fig. 1E; data not shown). Quantification showed that 100% of Nkx2.2+ (p3) and FoxA2+ (FP) cells were also β-gal+ (n=15 sections from six animals). Thus, the *Nkx2.2 p3*-CRM is initially activated in three progenitor pools but expression persists only in the p3 domain. By contrast, 89% of Olig2+ pMN cells co-expressed β-gal, whereas 11% did not (n=8 sections from six animals). These data are consistent with prior expression studies showing that Olig2 expression is activated in advance of Nkx2.2 in some ventral progenitors (Jeong and McMahon, 2005) and reveals that only a subset of cells uniquely activate Olig2.

We also examined β-gal expression in embryos from *FoxA2*$^{FP\text{-}CRM}$*::Cre* × *ROSA26*^{flxlz} crosses. β-gal was detected in FP cells that co-expressed endogenous FoxA2 and Shh and some cells at the FP/p3 border that express Nkx2.2 weakly (Fig. 1F,G; data not shown). These results, taken with prior published lineage analysis of reporter expression from an *Olig2:Cre* line (Dessaud et

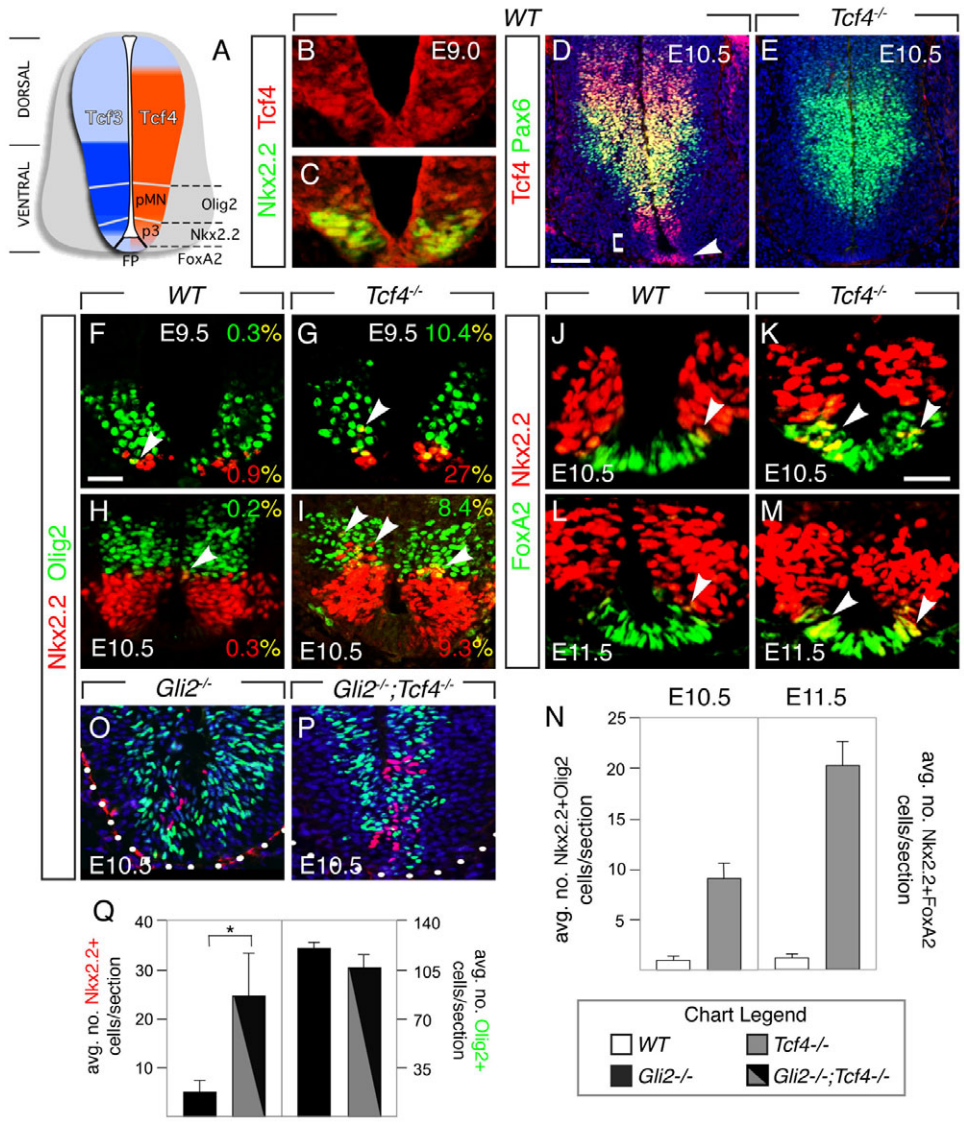

Fig. 2. Disrupted progenitor boundaries in *Tcf4* mutant embryos. (**A**) Schematic of Tcf3/Tcf4 expression in E10.5-11.5 mouse spinal cord. (**B**,**C**) Tcf4 protein expression at E9.0 is detected in presumptive Nkx2.2+ p3 cells and more dorsal cells. (**D**) At E10.5, Tcf4 is expressed in the ventral and dorsal ventricular zone (VZ) and in the FP (arrowhead in D), whereas weaker expression is detected in p3 cells (bracket) at this stage. The expression of Tcf4 and Pax6 overlap extensively in VZ cells along the dorsal ventral axis. (**E**) In *Tcf4* mutants, no Tcf4 protein expression is detected, but Pax6 expression persists. (**F-I**) Analysis of pMN/p3 boundary formation at E9.5 and E10.5 in *Tcf4* mutants using Nkx2.2 and Olig2 staining. Arrowheads indicate double-labeled cells. Percentages indicate the fraction of total Olig2 (green) or Nkx2.2 (red) cells that co-express both markers (i.e. yellow staining). (**J-M**) Analysis of p3/FP boundary formation at E10.5 and E11.5 in *Tcf4* mutants using Nkx2.2 and FoxA2 staining. In both cases, a greater number of double-labeled cells (yellow, arrowheads) can be detected primarily at the boundary region compared with wild type (WT). (**N**) Quantification of Nkx2.2/Olig2 and Nkx2.2/FoxA2 double-labeled cells. (**O-Q**) Analysis of Nkx2.2 p3 and Olig2 pMN cell specification in *Gli2 Tcf4* double-mutant embryos compared with single *Gli2* mutants. There is a significant increase in the number of Nkx2.2+ cells in double mutants compared with *Gli2* mutants alone (*P=0.0114, n=10 sections each in four to five embryos). Error bars represent s.e.m. Some sections counterstained with DAPI (blue). White dotted line indicates spinal cord margin. Scale bars: 50 μm in D,E; 25 μm in F-P.

al., 2007; Jeong and McMahon, 2005; Sun et al., 2006), support a model in which Nkx2.2 expression is activated in the progenitors to three distinct ventral lineages but becomes downregulated in two of these during domain segregation (Fig. 1H).

Tcf4 is required to maintain restricted Nkx2.2 expression in ventral progenitors

In wild-type (WT) mouse embryos at E10.5-11.5, Tcf4 expression in the VZ encompassed both dorsal and ventral regions (summarized in Fig. 2A). At E9.0, Tcf4 expression was detected in cells occupying approximately the ventral half of the neural tube (Fig. 2B,C; data not shown). Ventrally, Tcf4 was expressed in Olig2+ pMN progenitors, but was downregulated in Nkx2.2+ p3 progenitors between E9.0 and E10.5 (Fig. 2B-D). At these stages, Tcf4 expression overlapped extensively with Pax6, a protein that is required for p3/pMN boundary formation (Fig. 2D) (Ericson et al., 1997b). Tcf4 was also seen in floorplate (FP) cells at ~E9.5 (Fig. 2D).

To determine the requirement of Tcf4 in ventral patterning, we examined progenitor domain boundary formation in homozygous targeted *Tcf4*$^{-/-}$ embryos (Korinek et al., 1998) at E9.5-11.5. As

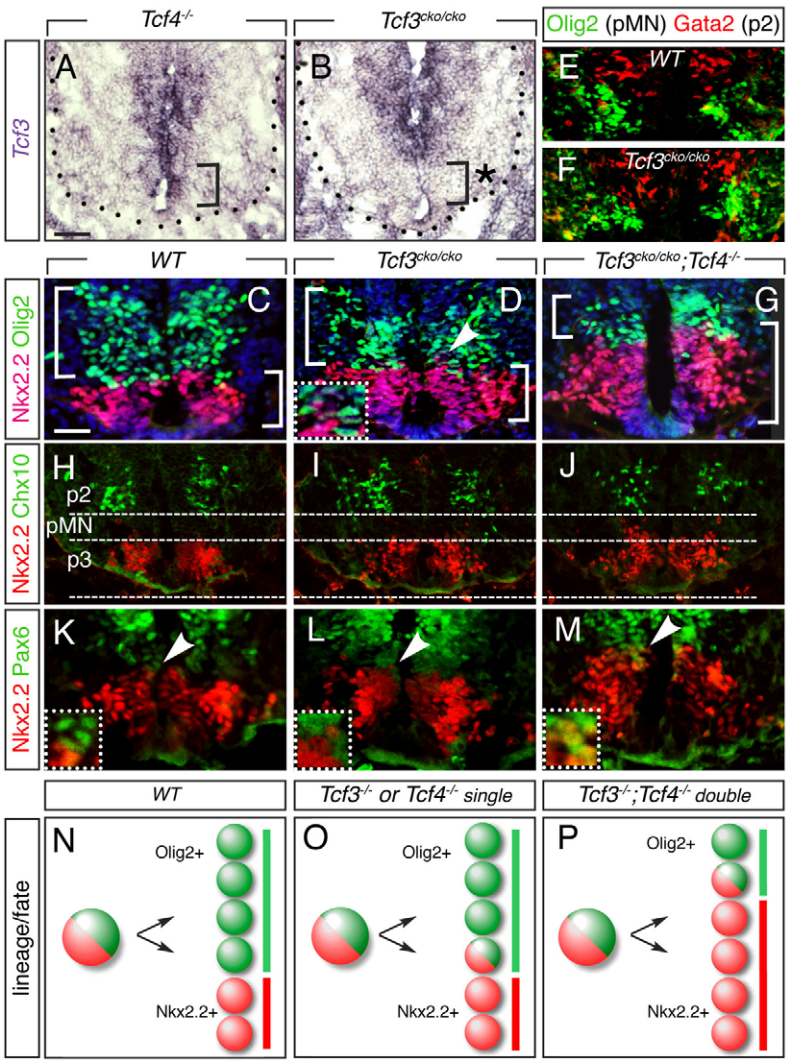

Fig. 3. *Tcf3* functions redundantly with *Tcf4* to control ventral progenitor patterning. (**A**,**B**) *Tcf3* mRNA expression in *Tcf4* and conditional *Tcf3* mutants (*Tcf3*$^{cko/cko}$) (generated in crosses with transgenic *Nkx2.2 p3*-CRM::*Cre* mice) at E10.75. Note the absence of *Tcf3* expression in p3 and pMN cells in *Tcf3*$^{cko/cko}$ embryo (brackets, asterisk). Black dotted line indicates the spinal cord margin. (**C**,**D**) Analysis of p3/pMN boundary formation in conditional *Tcf3*$^{cko/cko}$ and *Tcf3*$^{cko/cko}$*;Tcf4* double mutants at E10.5. A mild disruption is seen in *Tcf3*$^{cko/cko}$ mutants that is similar to that observed in single *Tcf4* mutants. Inset in D shows enlargement of area indicated by arrowhead. (**E**,**F**) Analysis of p2/pMN boundary formation in E10.5 conditional *Tcf3*$^{cko/cko}$ mutants using Gata2 and Olig2 staining. No differences were seen comparing WT with conditional *Tcf3* mutants. (**G**) In *Tcf3*/*Tcf4* double mutant embryos at E10.5, a dorsal expansion of Nkx2.2+ cells into the pMN domain is seen, along with a reduction in the number of Olig2+ pMN cells (brackets delineate the p3 domain in C,D,G). (**H-J**) Expression of Chx10 (V2 cells) and Nkx2.2 in WT, conditional *Tcf3*$^{cko/cko}$ and *Tcf3*$^{cko/cko}$*;Tcf4* double mutants at E10.5 showing a reduction in the pMN domain in double mutants. Lower line indicates ventral boundary of the spinal cord. (**K-M**) Co-expression of Pax6 and Nkx2.2 in E10.5 *Tcf3*$^{cko/cko}$*;Tcf4* double mutants but not WT or *Tcf3*$^{cko/cko}$ embryos. Inset shows enlargement of area indicated by arrowhead. (**N-P**) Model for changes in p3/pMN patterning based on lineage studies (Fig. 1) and mutant phenotypes. Scale bars: in A, 80 μm for A,B; in C, 40 μm for C-G and 60 μm for H-M.

expected (Korinek et al., 1998), no Tcf4 expression was seen in homozygous *Tcf4* mutants, whereas overall Pax6 expression was maintained (Fig. 2E), consistent with earlier data suggesting that Tcf4 functions downstream of Pax6 to regulate the p3/pMN boundary (Lei et al., 2006). Analysis of Olig2 and Nkx2.2 expression in *Tcf4*$^{-/-}$ mutants between E9.5 and E10.5 revealed ectopic Nkx2.2+ cells within the pMN domain, many co-expressing Olig2 (Fig. 2F-I,N). Neither the pMN/p2 boundary nor the generation of post-mitotic MNs or V0-V2 interneurons was affected, nor was the expression of cell cycle or general neuronal differentiation markers, indicating that the p3/pMN defects were not due to a non-specific negative effect on neurogenesis (see Figs S1-S3 in the supplementary material; data not shown). Analysis of the p3/FP boundary also revealed an increase in the number of Nkx2.2+ cells within the lateral FP, most or all of which co-expressed FoxA2 (Fig. 2J-M,O). These data show that Tcf4 is required for the proper formation of both the pMN/p3 and p3/FP progenitor boundaries.

To determine whether Shh signaling was affected in *Tcf4* mutants, we measured the expression of *Gli1* quantitatively using qRT-PCR. *Gli1* is a well-established direct target of Shh signaling that contains consensus binding sites for Gli, but not Tcf, proteins (Vokes et al., 2007). Consistent with the normal expression of Shh mRNA and protein in the FP of *Tcf4*$^{-/-}$ embryos, no differences were seen in *Gli1* mRNA levels compared with WT controls (see Fig. S3 in the supplementary material; data not shown). These data suggest that in the absence of Tcf4, endogenous Shh-Gli signaling is not sufficient to establish and maintain sharp pMN, p3 and FP domain boundaries.

Our previous studies showed that deletion of two Tcf sites in the *Nkx2.2 p3*-CRM results in ectopic reporter expression in more dorsal regions far from the ventral midline source of Shh, suggesting that the enhancer can respond to lower levels of endogenous GliA activity in the absence of Tcf binding (Lei et al., 2006). Therefore, it is possible that the changes in *Nkx2.2* expression seen in *Tcf4* mutants could partly be explained by an increase in the response of this gene to Shh resulting from a loss of Tcf4 repressor activity (i.e. de-repression). If this were the case, then the absence of Tcf4 under conditions of diminished Shh-Gli signaling should rescue Nkx2.2 expression. To test this, we analyzed Nkx2.2 expression in *Tcf4* homozygotes on the *Gli2* mutant background. Consistent with this possibility, Nkx2.2 expression was partially restored in *Gli2 Tcf4* double homozygotes, compared with *Gli2*$^{-/-}$ mutants in which Nkx2.2 expression was nearly absent (Fig. 2O-Q) (Matise et al., 1998). By contrast, the number of Olig2 cells was not significantly different in either genotype (Fig. 2O-Q). This result suggests that the activation of Nkx2.2 by the remaining weaker Gli1 and Gli3

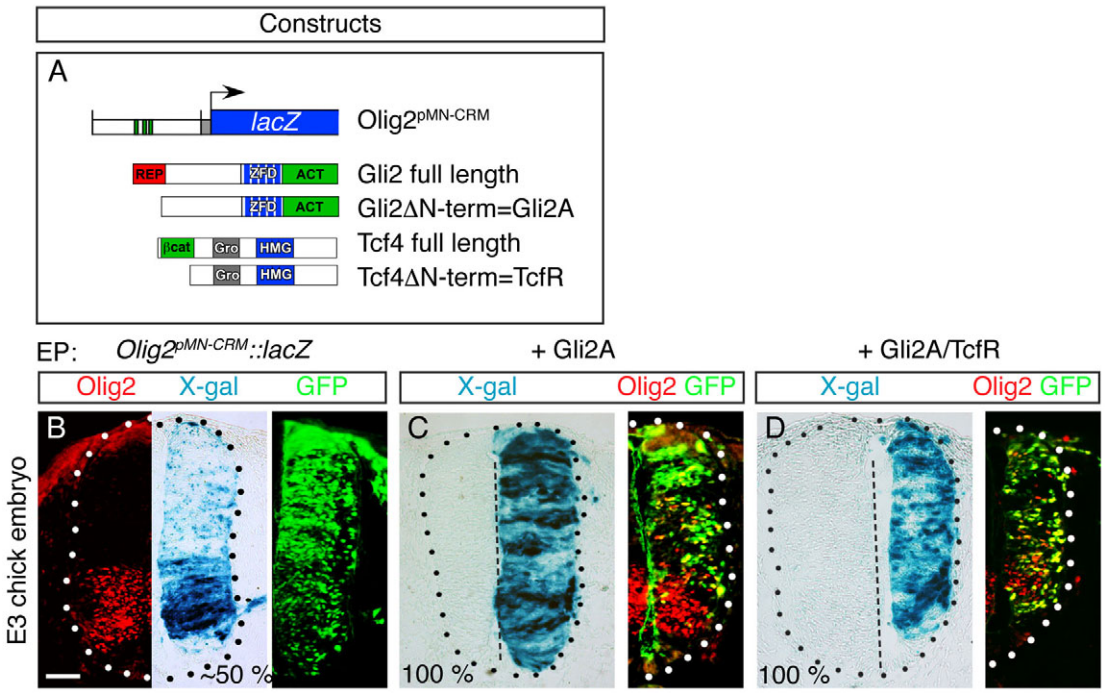

Fig. 4. An *Olig2*$^{pMN\text{-}CRM}$ is insensitive to Tcf regulation in vivo. (**A**) Schematic of constructs used. The 2.2-kb *Olig2 pMN*-CRM was cloned upstream of a minimal promoter (gray) and *lacZ* and contains three putative Gli binding sites (green boxes). ACT, activation; REP, repression; Gro, Grg/TLE binding; HMG, DNA binding; ZFD, zinc-finger domain. (**B**) Electroporation of a mouse *Olig2 pMN*-CRM driving *lacZ* (*Olig2*$^{pMN\text{-}CRM}$*::lacZ*) into the chick spinal cord at E2 results in restricted reporter expression in pMN cells marked by endogenous Olig2 expression at E3. (**C**) Co-transfection of Gli2A with the *Olig2*$^{pMN\text{-}CRM}$*::lacZ* construct results in the cell autonomous induction of β-gal expression throughout the transfected side of the neural tube. (**D**) Co-transfection of Gli2A + TcfR with the *Olig2*$^{pMN\text{-}CRM}$*::lacZ* construct does not block the induction of β-gal expression. Each panel comprises data from near-adjacent sections. Dotted lines indicate the spinal cord margin and central canal. Percentages indicate the proportion of embryos in which the phenotype was observed (see text for further details). Scale bar: 50 μm.

activators (Bai and Joyner, 2001) is normally masked in *Gli2* mutants by the inhibitory effect of Tcf4, and supports the idea that the loss of Tcf4 sensitizes *Nkx2.2* to positive Gli signaling.

Overlapping function of Tcf3 and Tcf4 in ventral patterning

Our lineage studies suggest that the patterning defects in *Tcf4*$^{-/-}$ embryos could be explained by a failure to downregulate or maintain repression of Nkx2.2 in the pMN and FP lineages. However, only a subset of cells within these domains is affected. Furthermore, our results indicate that Tcf4 functions downstream of Pax6, yet the dorsal expansion of Nkx2.2 in *Pax6* mutants is substantially worse than in *Tcf4* mutants (Ericson et al., 1997b). As *Tcf3* is also expressed in ventral neural progenitors and its expression was not altered in *Tcf4*$^{-/-}$ embryos (Fig. 3A), and both Tcf3 and Tcf4 can recognize the same DNA binding site (Clevers and van de Wetering, 1997), it is possible that Tcf3 could function redundantly with Tcf4 in ventral neural progenitors.

To test this, we first generated embryos with selective *Tcf3* inactivation in the FP, p3 and pMN domains using a conditional floxed *Tcf3* allele (Nguyen et al., 2009) and our *Nkx2.2*$^{p3\text{-}CRM}$*::Cre* line, which drives expression in most cells within these three lineages (Fig. 1H). Successful deletion of *Tcf3* was confirmed by loss of mRNA expression in conditional mutants (*Tcf3*$^{cko/cko}$) (Fig. 3A,B). Analysis of pMN/p3 boundary formation in *Tcf3*$^{cko/cko}$ embryos at E10.5 revealed ectopic Nkx2.2+ cells within the pMN domain, some of which co-expressed Olig2 (Fig. 3C,D; see Fig. S5 in the supplementary material), a phenotype that is similar to but milder than *Tcf4* mutants. No patterning defects were seen in the FP (which does not express detectable levels of *Tcf3*) or in the p2 domain (which does not express Cre) (Fig. 3E,F; see Fig. S3 in the supplementary material; data not shown), showing that the defect occurs only in cells lacking *Tcf3* expression.

We next generated conditional *Tcf3 Tcf4* double mutant embryos to determine their possible redundancy. Consistent with this, there was a significant expansion of Nkx2.2+ cells into the pMN domain in 44% of the double mutants examined ($n \geq 9$ sections from four embryos) compared with single mutants at E10.5 (Fig. 3G). This was accompanied by a reduction in Olig2+ pMN cells and in the gap between Nkx2.2+ and Chx10+ V2 cells at E10.5 (Fig. 3H-J). At E11.5, there were also fewer Isl1+ motoneurons in thoracic regions in double mutants (see Fig. S3 in the supplementary material). These findings show that both *Tcf3* and *Tcf4* are required to control the p3-restricted expression of Nkx2.2, and suggest that in their absence many cells fated to become Olig2+ pMN cells switch to an Nkx2.2+ 'p3' fate (Fig. 3N-P). Notably, Nkx2.2+ cells within the pMN domain co-expressed Pax6 in some double mutants, unlike WT embryos or single *Tcf3* or *Tcf4* mutants in which these two factors formed a sharp boundary at the pMN/p3 domains (Fig. 3K-M) [mean 1±0.3 vs 8±0.9 co-labeled cells in WT vs double mutants, respectively; n=10 and 17 sections, respectively, from four embryos each]. These results suggest that Pax6 can no longer fully repress Nkx2.2 expression in the absence of both *Tcf3* and *Tcf4*, supporting the idea that these factors function jointly to regulate pMN/p3 boundary formation downstream of Pax6 (Lei et al., 2006).

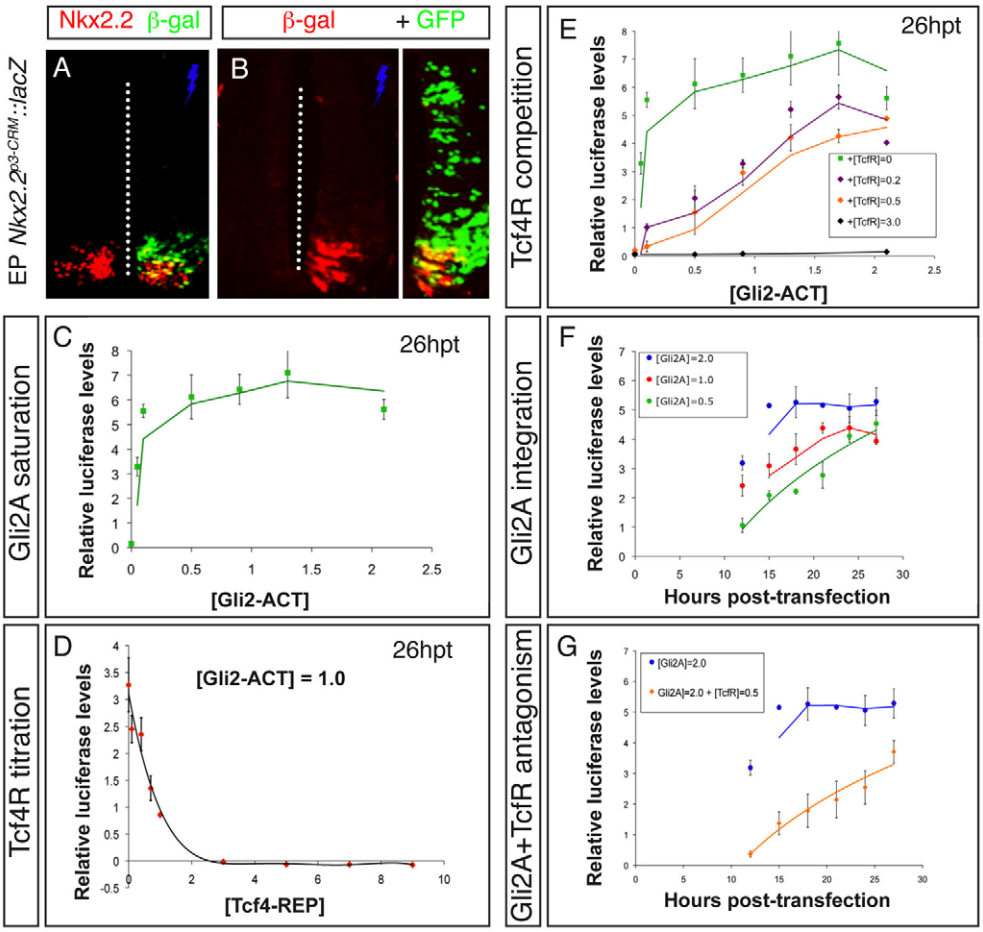

Fig. 5. Tcf repressor activity alters the Gli-induction kinetics of the *Nkx2.2 p3* CRM. (**A**,**B**) Electroporation of a mouse *Nkx2.2 p3*-CRM driving *lacZ* (*Nkx2.2*$^{p3\text{-}CRM}$*::lacZ*) into the chick spinal cord at E2 results in restricted reporter expression in p3 cells at E3. Dotted line indicates central canal. (**C-G**) Plots of relative luciferase levels driven by the *Nkx2.2 p3*-CRM (*Nkx2.2*$^{p3\text{-}CRM}$*::luciferase*). (C) Co-transfection of increasing concentrations of Gli2A saturates luciferase reporter response below 1 μg/μl when assayed at 26 hours post-transfection (hpt). (D) Co-transfection of increasing concentrations of Tcf4R with the *Nkx2.2*$^{p3\text{-}CRM}$*::luciferase* reporter at a constant level (1 μg/μl) of Gli2A can antagonize reporter activity in a graded manner. (E) Comparison of *Nkx2.2*$^{p3\text{-}CRM}$*::luciferase* activity at various levels of Gli2A and Tcf4R. Low (purple diamonds), intermediate (orange diamonds) and high (black diamonds) TcfR levels were tested against the Gli2A levels given on the *x*-axis. (F) Measurements of luciferase activity over a 12-27 hour time period at three different Gli2A concentrations (high, dark blue dots; intermediate, red dots; low, green dots) indicates that the *Nkx2.2 p3*-CRM integrates its response over time. (G) Measurements of luciferase activity over a 12-27 hour time period at a constant level of Gli2A (2 μg/μl) in the presence of an intermediate level ofTcf4R (orange diamonds) shows that Tcf4R can alter the temporal response of the enhancer to positive Gli2A input in a manner similar to lowering the level of Gli2A by ~75% (compare with F). The high level (2.0 μg/μl) Gli2A curve (blue dots) has been reproduced from F to allow direct comparison. Error bars represent s.e.m.

Tcf repressor activity selectively elevates the Gli activation threshold for Nkx2.2 but not Olig2

Our results above provide genetic evidence that Tcf transcription factors are required to repress Nkx2.2 expression in the pMN lineage, and indicate that Nkx2.2 and Olig2 are differentially sensitive to Tcf repressor activity. To test this, we asked whether the *Olig2*$^{pMN\text{-}CRM}$ element could be regulated by Tcf input in vivo. Transfection of the *Olig2*$^{pMN\text{-}CRM}$ construct (*Olig2*$^{pMN\text{-}CRM}$*::lacZ*) (Fig. 4A) resulted in β-gal expression that was confined to the Olig2+ pMN domain in ~50% of transfected embryos (*n*=9) (Fig. 4B). The remaining 50% of embryos either had no reporter expression or ectopic activity in roughly equal parts (data not shown). To test whether TcfR could regulate *Olig2*$^{pMN\text{-}CRM}$*::lacZ*, we assayed whether Gli-induced reporter expression could be blocked by a dominant-negative Tcf construct (Tcf4R) (Fig. 4A) (Megason and McMahon, 2002). In co-transfected embryos, β-gal expression was widespread along the DV axis, similar to Gli2A-alone transfected embryos (Fig. 4C,D). Although we cannot rule out the possibility that Tcf/Lef factors could influence *Olig2* expression via distinct regulatory elements (Sun et al., 2006), these results indicate that the pMN-specific expression of Olig2 is not influenced by TcfR in the context of the *Olig2*$^{pMN\text{-}CRM}$ enhancer, and are consistent with data showing that endogenous Olig2 expression is not affected when TcfR activity is altered in vivo as well as with preliminary ChIP data indicating that Tcf3/4 proteins do not bind the *Olig2*$^{pMN\text{-}CRM}$ enhancer in vivo (data not shown).

The above findings provide genetic evidence that the repressive influence of Tcf4 might function to elevate the threshold level of positively acting Gli proteins (GliA) required to induce expression of Nkx2.2, but has no effect on Olig2 expression. To test this directly, we employed an in vivo assay to compare the induction of *luciferase* expression driven by the *Nkx2.2 p3*-CRM (*Nkx2.2*$^{p3\text{-}CRM}$*::luciferase*)

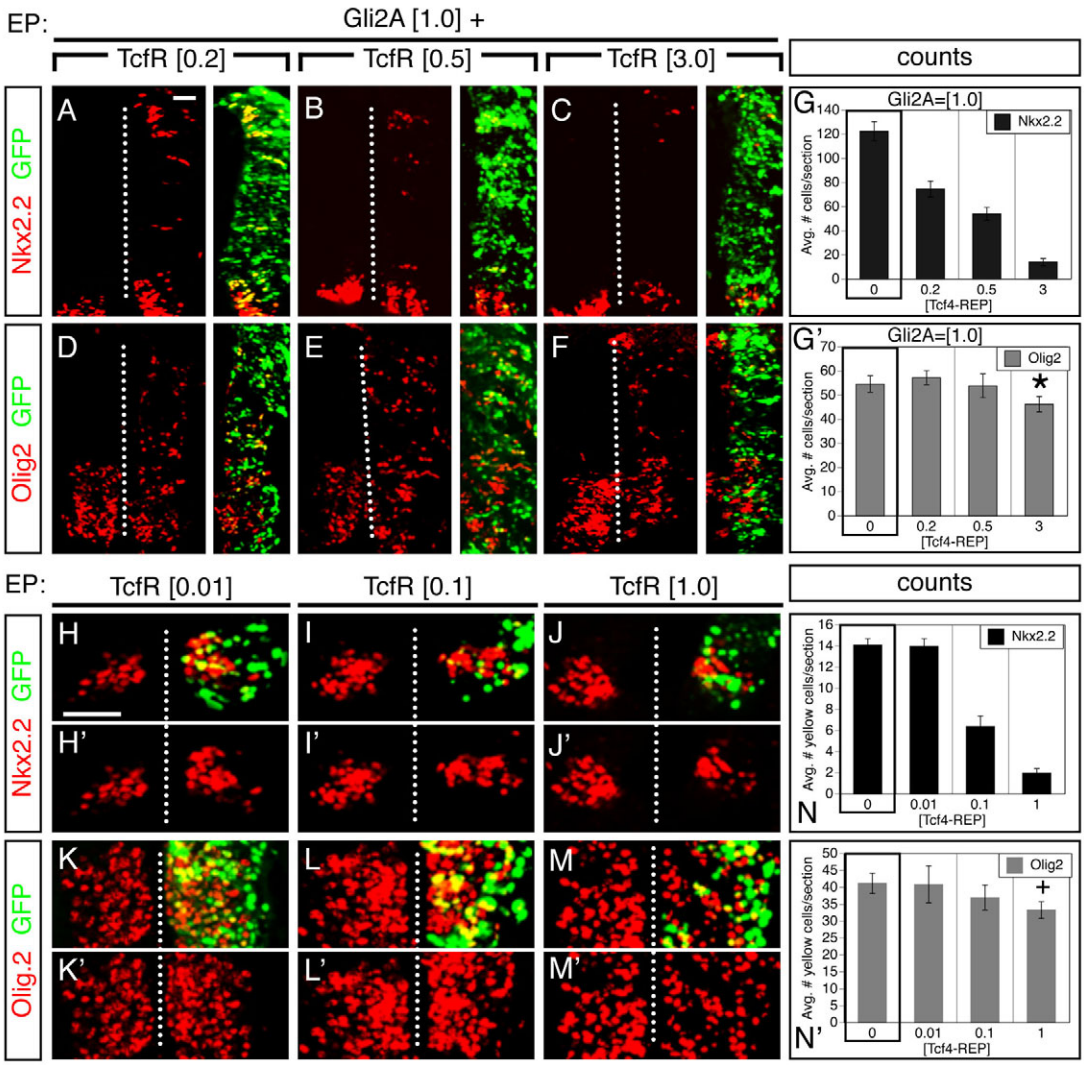

Fig. 6. Graded inhibition of Gli2A induction of Nkx2.2 by TcfR in vivo. (**A-F**) Sections through E3 chick embryos transfected on E2 with the indicated constructs and stained for either Nkx2.2 or Olig2 in red. Inset to right of each figure shows co-transfected GFP. (**G**,**G'**) Increasing concentrations of Tcf4R can antagonize the induction of Nkx2.2 by Gli2A, but has no effect on Olig2. (**H-N'**) Transfection of increasing amounts of Tcf4R into the p3 domain can progressively suppress endogenous Nkx2.2 expression here, but has no significant effect on the expression of Olig2 in the pMN domain. Graphs include control transfection data not shown in image panels for comparison ('0' values outlined by box: Gli2A alone for G,G' and GFP alone for N,N'). **P*=0.0743, $^{+}$*P*=0.052, both compared with controls. Dotted lines indicate central canal. Error bars represent s.e.m. Scale bars: 50 μm.

in the presence of TcfR. Transfection of the *Nkx2.2 p3*-CRM (*Nkx2.2*$^{p3\text{-}CRM}$*::lacZ*) driving *lacZ* in the chick spinal cord showed p3-restricted expression in 86% of the embryos examined (*n*=7) (Fig. 5A,B), indicating that the regulation of this enhancer is similar in both transgenic mouse and transfected chick systems.

We first characterized the response of the *Nkx2.2 p3*-CRM to graded levels of Gli activator by holding the concentration of the *Nkx2.2*$^{p3\text{-}CRM}$*::luciferase* construct constant and transfecting increasing amounts of Gli2A. As the concentration of Gli2A was increased, luciferase reporter activity initially increased rapidly but then leveled off at ~1 μg/μl, and higher concentrations did not induce additional activity (Fig. 5C). We next examined the concentration range over which Tcf4R could inhibit Gli2A. For this, we co-transfected increasing concentrations of Tcf4R with a fixed level of Gli2A from the low end of the saturation curve obtained from experiments in Fig. 5C. We found that Tcf4R could inhibit Gli2A-stimulated *Nkx2.2*$^{p3\text{-}CRM}$*::luciferase* expression proportional to the level of Tcf4R, up to a point at which expression was completely inhibited (Fig. 5D), indicating that Tcf4R can antagonize Gli2A activity in a concentration-dependent manner. To examine the effect of Tcf4R on Gli2A-induced reporter activity further, we co-transfected Tcf4R at a fixed level while increasing the concentration of Gli2A. We repeated this with three distinct Tcf4R levels spanning the range established by experiments in Fig. 5D. We found that for intermediate Tcf4R levels, four- to sixfold higher concentrations of Gli2A were required to induce a similar level of *Nkx2.2*$^{p3\text{-}CRM}$*::luciferase* activity, when measured at 26 hpt (Fig. 5E). Thus, the presence of Tcf4R can elevate the threshold concentration of Gli2A required to induce expression through the *Nkx2.2 p3*-CRM.

To determine whether there was a temporal component to the response, we transfected Gli2A at three different fixed concentrations and measured luciferase levels at 3-hour intervals between 12 and 27 hpt. Notably, lower concentrations of Gli2A

took longer to saturate the *Nkx2.2*$^{p3\text{-}CRM}$*::luciferase* response, such that the peak level was reached at a later time (Fig. 5F). These results show that the *Nkx2.2 p3*-CRM integrates its response to Gli2A proteins over time and as a function of initial concentration. Next, we co-transfected Gli2A along with Tcf4R at an intermediate level as determined in the experiments in Fig. 5E and measured *Nkx2.2*$^{p3\text{-}CRM}$*::luciferase* activity over the same time interval. In this case, the presence of Tcf4R shifted the enhancer response curve in a manner similar to lowering the level of Gli2A by ~75% (Fig. 5G). Thus, the presence of Tcf4R increases both the concentration and the length of time needed for Gli2A to activate *Nkx2.2 p3*-CRM expression.

Concentration-dependent repression of endogenous Nkx2.2 expression by Tcf-repressors

To assay directly whether Tcf4R can exert a similar differential negative effect on endogenous *Nkx2.2* and *Olig2* expression, we co-transfected Gli2A and Tcf4R and monitored induction of Nkx2.2 and Olig2 proteins. Transfection of increasing levels of Gli2A elicited a proportional induction of Nkx2.2+ cells in the neural tube (see Fig. S4 in the supplementary material). Similarly, Olig2+ cells were also induced in proportion to Gli2A concentration (see Fig. S4 in the supplementary material). Based on these results, we transfected an intermediate concentration of Gli2A with increasing levels of Tcf4R. The number of ectopic Nkx2.2+ cells decreased in proportion to increasing levels of Tcf4R (Fig. 6A-C), whereas the induction of Olig2+ cells was not affected (Fig. 6D-G). Thus, as with the *Nkx2.2 p3*-CRM, Tcf4R activity can inhibit endogenous Nkx2.2 induction by Gli2A in a concentration-dependent manner. Finally, we tested whether Tcf4R could have a similar effect on endogenous Nkx2.2 by transfecting increasing concentrations and assaying the number of transfected GFP+ cells that co-expressed Nkx2.2 in the p3 domain. We found that at the lowest Tcf4R levels, Nkx2.2 was not inhibited, whereas at higher levels there was a significant decrease in the number of transfected cells that expressed Nkx2.2 (Fig. 6H-J). No significant effect was seen on Olig2+ cells within the pMN domain at any Tcf4R level tested, indicating that these results were not due to a general inhibition of cell proliferation (Fig. 6K-N). These results show that Tcf4R can modulate the expression of Nkx2.2 in vivo and, together with mouse data, are consistent with the idea that the inhibitory influence of Tcf4 on Nkx2.2 serves to elevate selectively the threshold level of GliA needed to activate its expression.

DISCUSSION

A fundamental aspect of patterning and cell fate specification by morphogen signaling is that responses must be precisely regulated in both space and time to enact specific genetic programs in the dynamic cellular environment of developing embryos. Results from the current study show that differential inhibition of Shh-Gli target gene responses by Tcf/Lef repressors plays an important role in establishing distinct Shh-mediated cell fate programs in the spinal cord. This mechanism functions to restrict the fate choice among cells that will differentiate along distinct lineages but progenitors of which initially respond to similar levels of Shh-Gli signaling.

A role for Tcf proteins in regulating the patterned genetic response to Shh-Gli signaling

Our data provides several lines of evidence supporting the idea that Tcf3/4 repressors selectively elevate the threshold level of Shh-Gli signaling necessary to induce Nkx2.2 expression. First, reporter expression driven by an *Nkx2.2 p3*-CRM can be activated in the pMN domain and more dorsal cells when all Tcf repressor influences are removed, as in *Tcf3/4* mutants or transgenic reporter mice generated from an *Nkx2.2 p3* enhancer lacking only Tcf (but not Gli) binding sites (Lei et al., 2006). Second, Nkx2.2 expression is partially rescued in *Gli2 Tcf4* double mutants, suggesting that the weaker Gli1-Gli3 activators are sufficient to induce Nkx2.2 but only when TcfR levels are genetically reduced. Third, in vivo co-transfection assays demonstrate that the presence of TcfR elevates both the time and concentration of Gli2A necessary to induce *Nkx2.2 p3*-CRM-driven luciferase expression, and can also exert a graded negative influence over Gli2A-mediated induction of endogenous Nkx2.2. Finally, TcfR activity has no effect on endogenous Olig2 expression and cannot bind to or repress the expression of an *Olig2 pMN*-CRM.

Our data does not rule out the possibility that Tcf/Lef proteins could regulate Olig2 expression at higher levels or through independent regulatory elements (Sun et al., 2006) or via a more complex indirect mechanism. Prior studies using similar in vivo approaches showed that transfection of N-terminally truncated Tcf3 and Tcf4 proteins induced a broad dorsal expansion of ventral progenitor genes, including both *Nkx2.2* and *Olig2*, accompanied by a downregulation of dorsal genes such as *Pax6* and *Pax7* (Alvarez-Medina et al., 2008). Our transfection data showing that Olig2 is insensitive to TcfR activity appear to contradict these results, suggesting that subtle but significant details in experimental design and/or analysis could produce these differing results, such as final cDNA concentrations and embryo staging. Further detailed comparison between the specific methodologies used in each case will be necessary to resolve this issue.

Graded Shh-Gli signaling in the ventral neural tube

Results from our study suggest that distinct mechanisms exist for regulating the threshold responses of Shh-Gli target genes that are primarily controlled by GliA activation or GliR de-repression. Specifically, our data demonstrate that many or most cells at the DV position of the pMN domain continue to be exposed to a level of Shh-Gli activity sufficient to induce Nkx2.2 throughout neurogenesis, and that differential Gli levels across the p3/pMN boundary are insufficient to establish its restricted expression pattern. These results suggest that a putative GliA gradient might not be the sole or predominant source of patterning information in the ventral neural tube, and that the restricted response(s) of positively regulated target genes requires additional, potentially independent transcriptional input. Our data also raise the possibility that other Shh-Gli target genes that also require direct Gli activation employ a similar selective repressor strategy to restrict their responses to specific target fields.

Results from the current study provide further support for our model that Tcf3 and Tcf4 function downstream of Pax6 to regulate Nkx2.2 expression at the pMN/p3 boundary. However, because the dorsal expansion of Nkx2.3 in *Pax6* mutants is more severe than in compound *Tcf3/4* mutants, it is also possible that Pax6 controls additional negative regulators of Nkx2.2. A straightforward explanation for this is that our method for generating conditional *Tcf3/4* double mutants does not test its requirement dorsal to the pMN domain as the Cre driver used (the *Nkx2.2 p3*-CRM element) is only expressed in FP, p3 and pMN cells. However, recent evidence suggests that Pax6 controls *Gli3* expression (Lek et al., 2010) raising the possibility that Pax6 opposes Shh target gene activation via both TcfR and GliR. If this were the case, then a possible role for Gli3 in negatively regulating Nkx2.2 would only

be revealed in the absence of *Tcf3/4*, because loss of *Gli3* on its own does not affect pMN/p3 boundary formation (Persson et al., 2002). Furthermore, as *Gli3* expression is not altered in *Tcf3/4* mutants (data not shown), the genetic programs would be likely to operate in parallel downstream of Pax6. However, as Shh signaling negatively regulates Pax6, which is required for normal *Tcf3/4* expression (Lei et al., 2006), the role of Tcf3/4 in neuronal patterning might not be completely independent of Shh.

Gene regulation during progenitor lineage segregation and domain consolidation

Our lineage data from the *Nkx2.2$^{p3\text{-}CRM}$::Cre* line at E10.5 indicate that the majority of cells within the pMN and FP domains derive from progenitors that had transiently activated Nkx2.2 expression, except for ~10% of the Olig2+ pMN cells. This is consistent with published studies that showed that Olig2 expression is detected about 3-6 hours in advance of Nkx2.2 and that early co-expression of these proteins can be detected in some ventral midline progenitors (Dessaud et al., 2007; Jeong and McMahon, 2005). Taken in this context, our observations that Nkx2.2+ cells increase in number at the expense of Olig2+ cells in *Tcf3/Tcf4* double mutants suggests that many cells normally fated to become Olig2+ pMN cells fail to properly downregulate or maintain suppression of Nkx2.2 in this lineage, resulting in a partial cell fate switch reflected by the reduction in Isl1+ motoneurons at E11.5. By contrast, the overall numbers of Nkx2.2+ and Olig2+ cells are not significantly altered in single *Tcf3* and *Tcf4* mutants, although there are more cells co-expressing Nkx2.2 and Olig2 in these lines compared with both normal littermates and *Tcf3 Tcf4* double mutants. One possible explanation for this difference is that in both *Tcf3* and *Tcf4* single mutants the level of ectopic Nkx2.2 is insufficient to repress Olig2, possibly owing to the lingering negative effect of the remaining Tcf3 or Tcf4 proteins on Nkx2.2 expression. Our data does not rule out the possibility that additional mechanisms contribute to the relative timing of Olig2 and Nkx2.2 induction in ventral progenitors or their subsequent segregation into the pMN and p3 domains. For example, it is possible that Gli proteins independently regulate target genes that play a role in progenitor cell sorting (Lei et al., 2004) or cell cycle progression (Cayuso et al., 2006). Therefore, a combination of both Gli-specific induction mechanisms and selective Tcf repression is likely to contribute to the temporal and spatial pattern of gene induction and domain segregation.

Regulation of Tcf activity in ventral progenitors

Tcf3 and Tcf4 belong to the Tcf/Lef family of HMG-box transcription factors that have been linked to Wnt signaling (Hurlstone and Clevers, 2002; Nusse, 1999). Tcf/Lef proteins, like Gli proteins, can either activate or repress target genes depending on signaling status. However, one difference is that the transcriptional activity of Tcf proteins is mediated by association with distinct co-factors, such as β-catenin, and not proteolytic processing from a longer precursor (Hurlstone and Clevers, 2002; Nusse, 1999). In the developing CNS, activation of the Wnt/β-catenin pathway can promote progenitor cell cycle progression and inhibit differentiation (Cayuso and Marti, 2005; Megason and McMahon, 2002; Sommer, 2004). These effects are likely to be mediated through direct control of cell-cycle target genes, such as Cyclin D1 and/or *N/C-Myc* (Clevers, 2006). Furthermore, although the primary influence of canonical Wnt signaling appears to be in the dorsal spinal cord in accord with the expression of multiple Wnt ligands in this region (Bonner et al., 2008; Chesnutt et al., 2004; Gribble et al., 2009; Ille et al., 2007; Muroyama et al., 2002), several studies have shown that Wnt signaling can also influence the differentiation of ventral neuronal cell types in opposition to Shh, perhaps via regulation of *Gli3* (Alvarez-Medina et al., 2008; Alvarez-Medina et al., 2009; Robertson et al., 2004; Yu et al., 2008). By contrast, our analysis did not reveal any changes in Cyclin D1 (Ccnd1) expression or general alterations in cell proliferation and differentiation in the dorsal spinal cord of *Tcf4* mutants or ventrally in *Tcf3/4* double mutants. As these are the only identified Tcf/Lef factors expressed in ventral progenitors, our findings call into question the model in which all positive Wnt/β-catenin signaling is transduced through Tcf/Lef proteins and these proteins are dedicated mediators of the Wnt pathway implementing its effect on cell proliferation and differentiation.

Acknowledgements

This research was supported by grants from the NIH/NICHD and NSF to M.P.M. Deposited in PMC for release after 12 months.

Competing interests statement

The authors declare no competing financial interests.

Supplementary material

Supplementary material for this article is available at
http://dev.biologists.org/lookup/suppl/doi:10.1242/dev.068270/-/DC1

References

Alvarez-Medina, R., Cayuso, J., Okubo, T., Takada, S. and Marti, E. (2008). Wnt canonical pathway restricts graded Shh/Gli patterning activity through the regulation of Gli3 expression. *Development* **135**, 237-247.

Alvarez-Medina, R., Le Dreau, G., Ros, M. and Marti, E. (2009). Hedgehog activation is required upstream of Wnt signalling to control neural progenitor proliferation. *Development* **136**, 3301-3309.

Bai, C. and Joyner, A. (2001). Gli1 can rescue the in vivo function of Gli2. *Development* **128**, 5161-5172.

Bai, C. B., Stephen, D. and Joyner, A. L. (2004). All mouse ventral spinal cord patterning by hedgehog is Gli dependent and involves an activator function of Gli3. *Dev. Cell* **6**, 103-115.

Bonner, J., Gribble, S. L., Veien, E. S., Nikolaus, O. B., Weidinger, G. and Dorsky, R. I. (2008). Proliferation and patterning are mediated independently in the dorsal spinal cord downstream of canonical Wnt signaling. *Dev. Biol.* **313**, 398-407.

Briscoe, J., Pierani, A., Jessell, T. M. and Ericson, J. (2000). A homeodomain protein code specifies progenitor cell identity and neuronal fate in the ventral neural tube. *Cell* **101**, 435-445.

Cayuso, J. and Marti, E. (2005). Morphogens in motion: growth control of the neural tube. *J. Neurobiol.* **64**, 376-387.

Cayuso, J., Ulloa, F., Cox, B., Briscoe, J. and Marti, E. (2006). The Sonic hedgehog pathway independently controls the patterning, proliferation and survival of neuroepithelial cells by regulating Gli activity. *Development* **133**, 517-528.

Chesnutt, C., Burrus, L. W., Brown, A. M. and Niswander, L. (2004). Coordinate regulation of neural tube patterning and proliferation by TGFbeta and WNT activity. *Dev. Biol.* **274**, 334-347.

Clevers, H. (2006). Wnt/beta-catenin signaling in development and disease. *Cell* **127**, 469-480.

Clevers, H. and van de Wetering, M. (1997). TCF/LEF factor earn their wings. *Trends Genet.* **13**, 485-489.

Dessaud, E., Yang, L. L., Hill, K., Cox, B., Ulloa, F., Ribeiro, A., Mynett, A., Novitch, B. G. and Briscoe, J. (2007). Interpretation of the sonic hedgehog morphogen gradient by a temporal adaptation mechanism. *Nature* **450**, 717-720.

Dessaud, E., McMahon, A. P. and Briscoe, J. (2008). Pattern formation in the vertebrate neural tube: a sonic hedgehog morphogen-regulated transcriptional network. *Development* **135**, 2489-2503.

Ericson, J., Thor, S., Edlund, T., Jessell, T. M. and Yamada, T. (1992). Early stages of motor neuron differentiation revealed by expression of homeobox gene *Islet-1*. *Science* **256**, 1555-1560.

Ericson, J., Briscoe, J., Rashbass, P., van Heyningen, V. and Jessell, T. M. (1997a). Graded sonic hedgehog signaling and the specification of cell fate in the ventral neural tube. *Cold Spring Harb. Symp. Quant. Biol.* **62**, 451-466.

Ericson, J., Rashbass, P., Schedl, A., Brenner-Morton, S., Kawakami, A., van Heynigen, V., Jessell, T. M. and Briscoe, J. (1997b). Pax6 controls progenitor cell identity and neuronal fate in response to graded Shh signaling. *Cell* **90**, 169-180.

Gribble, S. L., Kim, H. S., Bonner, J., Wang, X. and Dorsky, R. I. (2009). Tcf3 inhibits spinal cord neurogenesis by regulating sox4a expression. *Development* **136**, 781-789.
Hurlstone, A. and Clevers, H. (2002). T-cell factors: turn-ons and turn-offs. *EMBO J.* **21**, 2303-2311.
Ille, F., Atanasoski, S., Falk, S., Ittner, L. M., Marki, D., Buchmann-Moller, S., Wurdak, H., Suter, U., Taketo, M. M. and Sommer, L. (2007). Wnt/BMP signal integration regulates the balance between proliferation and differentiation of neuroepithelial cells in the dorsal spinal cord. *Dev. Biol.* **304**, 394-408.
Jacob, J. and Briscoe, J. (2003). Gli proteins and the control of spinal-cord patterning. *EMBO Rep.* **4**, 761-765.
Jeong, J. and McMahon, A. P. (2005). Growth and pattern of the mammalian neural tube are governed by partially overlapping feedback activities of the hedgehog antagonists patched 1 and Hhip1. *Development* **132**, 143-154.
Jessell, T. M. (2000). Neuronal specification in the spinal cord: inductive signals and transcriptional codes. *Nat. Rev. Genet.* **1**, 20-29.
Jiang, J. and Hui, C. C. (2008). Hedgehog signaling in development and cancer. *Dev. Cell* **15**, 801-812.
Korinek, V., Barker, N., Moerer, P., van Donselaar, E., Huls, G., Peters, P. J. and Clevers, H. (1998). Depletion of epithelial stem-cell compartments in the small intestine of mice lacking Tcf-4. *Nat. Genet.* **19**, 379-383.
Lee, S.-K. and Pfaff, S. L. (2001). Transcriptional networks regulating neuronal identity in the developing spinal cord. *Nat. Neurosci.* **4**, 1183-1191.
Lei, Q., Zelman, A. K., Kuang, E., Li, S. and Matise, M. P. (2004). Transduction of graded Hedgehog signaling by a combination of Gli2 and Gli3 activator functions in the developing spinal cord. *Development* **131**, 3593-3604.
Lei, Q., Jeong, Y., Misra, K., Li, S., Zelman, A. K., Epstein, D. J. and Matise, M. P. (2006). Wnt signaling inhibitors regulate the transcriptional response to morphogenetic Shh-Gli signaling in the neural tube. *Dev. Cell* **11**, 325-337.
Lek, M., Dias, J. M., Marklund, U., Uhde, C. W., Kurdija, S., Lei, Q., Sussel, L., Rubenstein, J. L., Matise, M. P., Arnold, H. H. et al. (2010). A homeodomain feedback circuit underlies step-function interpretation of a Shh morphogen gradient during ventral neural patterning. *Development* **137**, 4051-4060.
Litingtung, Y. and Chiang, C. (2000). Specification of ventral neuron types is mediated by an antagonistic interaction between Shh and Gli3. *Nat. Neurosci.* **3**, 979-985.
Matise, M. P. and Joyner, A. L. (1997). Expression patterns of developmental control genes in normal and *Engrailed-1* mutant mouse spinal cord reveal early diversity in developing interneurons. *J. Neurosci.* **17**, 7805-7816.
Matise, M. P., Epstein, D. J., Park, H. L., Platt, K. A. and Joyner, A. L. (1998). Gli2 is required for induction of floor plate and adjacent cells, but not most ventral neurons in the mouse central nervous system. *Development* **125**, 2759-2770.
McMahon, A. P., Ingham, P. W. and Tabin, C. J. (2003). Developmental roles and clinical significance of hedgehog signaling. *Curr. Top. Dev. Biol.* **53**, 1-114.
Megason, S. G. and McMahon, A. P. (2002). A mitogen gradient of dorsal midline Wnts organizes growth in the CNS. *Development* **129**, 2087-2098.
Mo, R., Freer, A. M., Zinyk, D. L., Crackower, M. A., Michaud, J., Heng, H. H.-Q., Chik, K. W., Shi, X.-M., Tsui, L.-C., Cheng, S. H. et al. (1997). Specific and redundant functions of *Gli2* and *Gli3* zinc finger genes in skeletal patterning and development. *Development* **124**, 113-123.
Muroyama, Y., Fujihara, M., Ikeya, M., Kondoh, H. and Takada, S. (2002). Wnt signaling plays an essential role in neuronal specification of the dorsal spinal cord. *Genes Dev.* **16**, 548-553.
Nguyen, H., Merrill, B. J., Polak, L., Nikolova, M., Rendl, M., Shaver, T. M., Pasolli, H. A. and Fuchs, E. (2009). Tcf3 and Tcf4 are essential for long-term homeostasis of skin epithelia. *Nat. Genet.* **41**, 1068-1075.
Novitch, B. G., Wichterle, H., Jessell, T. M. and Sockanathan, S. (2003). A requirement for retinoic acid-mediated transcriptional activation in ventral neural patterning and motor neuron specification. *Neuron* **40**, 81-95.
Nusse, R. (1999). WNT targets. Repression and activation. *Trends Genet.* **15**, 1-3.
Pan, Y. and Wang, B. (2007). A novel protein-processing domain in Gli2 and Gli3 differentially blocks complete protein degradation by the proteasome. *J. Biol. Chem.* **282**, 10846-10852.
Pan, Y., Bai, C. B., Joyner, A. L. and Wang, B. (2006). Sonic hedgehog signaling regulates Gli2 transcriptional activity by suppressing its processing and degradation. *Mol. Cell. Biol.* **26**, 3365-3377.
Persson, M., Stamataki, D., te Welscher, P., Andersson, E., Bose, J., Ruther, U., Ericson, J. and Briscoe, J. (2002). Dorsal-ventral patterning of the spinal cord requires Gli3 transcriptional repressor activity. *Genes Dev.* **16**, 2865-2878.
Pierani, A., Brenner-Morton, S., Chiang, C. and Jessell, T. (1999). A sonic hedgehog-independent, retinoid-activated pathway of neurogenesis in the ventral spinal cord. *Cell* **97**, 903-915.
Ribes, V. and Briscoe, J. (2009). Establishing and interpreting graded Sonic Hedgehog signaling during vertebrate neural tube patterning: the role of negative feedback. *Cold Spring Harb. Perspect. Biol.* **1**, a002014.
Robertson, C. P., Braun, M. M. and Roelink, H. (2004). Sonic hedgehog patterning in chick neural plate is antagonized by a Wnt3-like signal. *Dev. Dyn.* **229**, 510-519.
Ruiz i Altaba, A., Nguyen, V. and Palma, V. (2003). The emergent design of the neural tube: prepattern, SHH morphogen and GLI code. *Curr. Opin. Genet. Dev.* **13**, 513-521.
Sasaki, H. and Hogan, B. L. (1996). Enhancer analysis of the mouse HNF-3 beta gene: regulatory elements for node/notochord and floor plate are independent and consist of multiple sub-elements. *Genes Cells* **1**, 59-72.
Sommer, L. (2004). Multiple roles of canonical Wnt signaling in cell cycle progression and cell lineage specification in neural development. *Cell Cycle* **3**, 701-703.
Soriano, P. (1999). Generalized lacZ expression with the ROSA26 Cre reporter strain. *Nat. Genet.* **21**, 70-71.
Stamataki, D., Ulloa, F., Tsoni, S. V., Mynett, A. and Briscoe, J. (2005). A gradient of Gli activity mediates graded Sonic Hedgehog signaling in the neural tube. *Genes Dev.* **19**, 626-641.
Sun, T., Hafler, B. P., Kaing, S., Kitada, M., Ligon, K. L., Widlund, H. R., Yuk, D. I., Stiles, C. D. and Rowitch, D. H. (2006). Evidence for motoneuron lineage-specific regulation of Olig2 in the vertebrate neural tube. *Dev. Biol.* **292**, 152-164.
Vokes, S. A., Ji, H., McCuine, S., Tenzen, T., Giles, S., Zhong, S., Longabaugh, W. J., Davidson, E. H., Wong, W. H. and McMahon, A. P. (2007). Genomic characterization of Gli-activator targets in sonic hedgehog-mediated neural patterning. *Development* **134**, 1977-1989.
Wijgerde, M., McMahon, J. A., Rule, M. and McMahon, A. P. (2002). A direct requirement for Hedgehog signaling for normal specification of all ventral progenitor domains in the presumptive mammalian spinal cord. *Genes Dev.* **16**, 2849-2864.
Yu, W., McDonnell, K., Taketo, M. M. and Bai, C. B. (2008). Wnt signaling determines ventral spinal cord cell fates in a time-dependent manner. *Development* **135**, 3687-3696.